90° domain dynamics and relaxation in thin ferroelectric/ferroelastic films

Yachin Ivry,[1,*] Nan Wang,[1,2] DaPing Chu,[2] and Colm Durkan[1,†]
[1]*Nanoscience Centre, University of Cambridge, 11 JJ Thomson Avenue, Cambridge CB3-0FF, United Kingdom*
[2]*Electrical Engineering Division, University of Cambridge, 9 JJ Thomson Avenue, Cambridge CB3-0FA, United Kingdom*
(Received 28 September 2009; revised manuscript received 11 March 2010; published 25 May 2010)

We investigated the dynamics and relaxation of 90° domains in 60-nm-thick lead-zirconium titanate ($PbZr_{0.3}T_{0.7}O_3$) films, with enhanced piezoresponse force microscopy. We show that under opposite electric fie ld, ferroelectric domains are reversibly switched while ferroelastic domains reorganize in a nonreversible way. Moreover, we show that the relaxation-time constant of 90° domains is two orders of magnitude shorter than for the previously reported 180° domains relaxation. Furthermore, we demonstrate the influence of geometry and scale on the relaxation process. Finally, we propose a relaxation mechanism for ferroelastic-ferroelectric systems, with implications for devices based on these materials.

DOI: 10.1103/PhysRevB.81.174118 PACS number(s): 77.80.−e, 77.84.−s, 77.90.+k

I. INTRODUCTION

Ferroelectric materials, being functional materials, have found applications in very many fields. For example, ferroelectric-based memories are currently a leading candidate for nonvolatile, low-power devices[1] and are widely used in everyday technologies such as rf filters in telecommunications and medical imaging systems.[2,3] Although ferroelectricity has been extensively studied at both the macroscopic (>1 μm) and atomic scales (<1 nm),[4,5] the relationship between the behavior at these two scales is still poorly understood due to technical difficulties engaged with intermediate-scale investigations.[6] Several commercially relevant ferroelectrics are also ferroelastic. Ferroelastic domains spontaneously form to minimize the local stress. The domains consist of periodic parallel stripes of alternating (i) *a*- and *c*-crystallographic orientations (known as *polytwins*) and consequently (ii) in-plane and out-of-plane polarizations, respectively. Although it is known that ferroelasticity strongly influences ferroelectricity,[7] to date, very few simultaneous observations of both have been reported. We have recently reported on a study of ferroelastic domains and found that (i) polytwins tend to form cooperative structures of a finite size, which we have termed "bundles" and (ii) they align not parallel to the nearest grain boundary, so are influenced by the local geometry.[8] During the last few years, several independent studies have reported ferroelastic domain motion under an external electric field. Since the *c* domains of a polydomain give rise to the out-of plane polarization (i.e., ferroelectricity), there is a great desire to study their kinetics. Moreover, there is a continuing attempt to associate in-plane ferroelastic domain motion with the enhancement of the essentially out-of-plane ferroelectric-related phenomena that have been observed in recent years.[6,9–13] However, although it is known that ferroelastic domains move under an applied electric field, it is not yet clear what the driving mechanism is. Furthermore, it is also not yet known how the ferroelastic domain motion influences macroscopic ferroelectricity. Therefore, a time-dependent investigation of the simultaneous dynamics of ferroelectricity and ferroelasticity under an external field is timely.

To explore the dynamics of ferroelasticity as well as its interplay with ferroelectricity, we used enhanced-piezoresponse force microscopy[14] (E-PFM), which is based on conventional piezoresponse force microscopy[15,16] but utilizes the cantilever dynamics to enhance the image contrast. This allows high-resolution (up to ~1 nm) mapping of ferroelectric and ferroelastic domains simultaneously with the topography.

We chose thin polycrystalline tetragonal piezoelectric (PZT) films for this study (60 nm thick, predominantly (110), similar to the films discussed elsewhere[14,17]) as PZT has the highest electromechanical coupling of any known material, so lends itself well to PFM investigations. The granularity of the films provides a simple way of exploring the effect of local geometry on ferroelectricity and ferroelasticity.

II. E-PFM AND LOCAL DOMAIN SWITCHING

E-PFM has been described elsewhere[8,14] and is similar to conventional PFM with three differences—(i) soft cantilevers are used; (ii) the magnitude of the ac drive voltage is larger, and (iii) the cantilever is driven close to its in-contact resonant frequency. The use of soft cantilevers leads to an additional electrostatically induced parabolic bending of the lever toward the sample surface but this is minimal[18] when compared to the deflection due to the piezoelectric deformation of the sample. The resultant force on the cantilever due to both sources of deflection is on the order a few tens of picometers and if the overall force for atomic force microscopy (AFM) imaging is kept low enough (<1 nN) the in-contact resonance frequency is approximately 4.4 times larger than the free resonance frequency.[19] That is, the cantilever does not act like one that is firmly clamped at both ends. It is important to note that the position of the resonance frequency and its dependence on the nature of the contact can be explained in a simple way.[20] Consider the cantilever as a point mass m^* connected to a spring of spring constant k. The resonance frequency of the free cantilever obeys: $f_{free}^2 = 4\pi^2 k/m^*$. In contact mode AFM, the forces acting on the tip are repulsive and therefore the spatial derivative of this force, k^* is negative. As a result, the resonance frequency of the cantilever that is in contact increases $(f_{1res}^{ic})^2 = 4\pi^2(k$

$-k^*)/m^*$. Substituting $k=0.2$ N/m and $f_{free}=13$ kHz gives rise to an effective mass of the cantilever of $m^* \approx 4.7 \times 10^{-8}$ kg. Substituting now $f_{1res}^{ic}=59.5$ kHz,[14] the effective tip-surface force derivative can be extracted: $k^* \approx -4$ N/m, i.e., $|k^*| \gg k$.

Factor (iii) above simply enhances the oscillation amplitude of the cantilever, whereas the operation frequency is chosen so that the oscillations are linear with the driving ac field, assuring the signal is piezoresponse. The primary consequence of this is that the signal-to-noise ratio of the PFM signal is greatly increased relative to the case of standard PFM, so the contrast associated with ferroelastic domains is more apparent. The use of a soft cantilever gives rise to a decrease in the effective tip-surface contact area. That is, a reduction in the friction and adhesion, and hence this can explain the increase in the imaging resolution. Moreover, the low stiffness of the cantilever protects the tip from wearing out during the experiments and hence from deteriorating the imaging. The resultant shearing motion of the tip on the sample (the electrostatic force causes the tip to tilt) leads to irregular oscillations if (a) the drive amplitude is too large, (b) the sample is very rough, or (c) the contact force is too large, which is why the vast majority of PFM is carried out well below this in-contact resonance frequency. The resonance frequency can vary significantly during imaging (by several kilohertz) due to variations in the local elastic modulus but we have not found this to be an issue, presumably due to the soft contact we are using and to operation in the regime of linear electromechanical response. For the samples we investigated, the optimum conditions for steady oscillation of the cantilever are 3–6 Vrms between the tip and sample. To validate the method, in Figs. 1(a)–1(c), we present topography, E-PFM amplitude and E-PFM phase of a large grain in the sample. Within this area, six roughly circular ferroelectric domains of diameter ~120 nm were formed by applying voltage pulses to the tip and the area was then imaged with E-PFM [Figs. 1(d)–1(f)]. In the phase image [Fig. 1(f)], the ferroelastic domains appear as gray parallel stripes (hereafter *c* orientation, although an in-plane component of the polarization in these areas is expected) separated by noisy regions (hereafter *a* orientation). The phase signal is highly unstable in the *a* regions as the cantilever oscillation is almost zero there, indicating that these stripes are separated by 90° domain walls. A schematic of the structure is brought in Fig. 1(g). The ferroelectric domains are clearly visible as bright spots and the line section through two of these that were taken from the same *c* domain stripe and is shown in Fig. 1(i) demonstrates that they are separated by 180° domain walls. By contrast, in the amplitude image [Fig. 1(e)], only the boundaries of ferroelectric domains are observed. This is due to the fact that in this stripe, both polarities of ferroelectric domain are still out of plane, so application of an ac voltage between the tip and sample will cause the sample and hence the tip to oscillate with the same amplitude by the inverse piezoelectric effect. The boundary appears as a dark line as expected. As can be seen from the line section in Fig. 1(i), the oscillation of the cantilever is symmetric for the two opposite out-of-plane domains and is very close to zero at the boundaries. This suggests that the electrostatic contribution to the cantilever oscillation is negligible, as was stated earlier. Another contribution to the cantilever oscillation amplitude that should be considered is the contact stiffness. Ferroelastic domains consist of alternating *a* and *c* crystallographic oriented regions, which will have different elastic moduli. Therefore, one may expect to obtain contrast in the amplitude image on the basis of this variation, as is the case in atomic force acoustic microscopy (AFAM).[20,21] However, this contrast should depend on the drive frequency and will switch sign depending on whether one is driving the cantilever above or below the resonance. We have found that the sign of the contrast we observe does not depend on frequency, indicating that variations in contact stiffness do not contribute to the imaging mechanism. Addi-

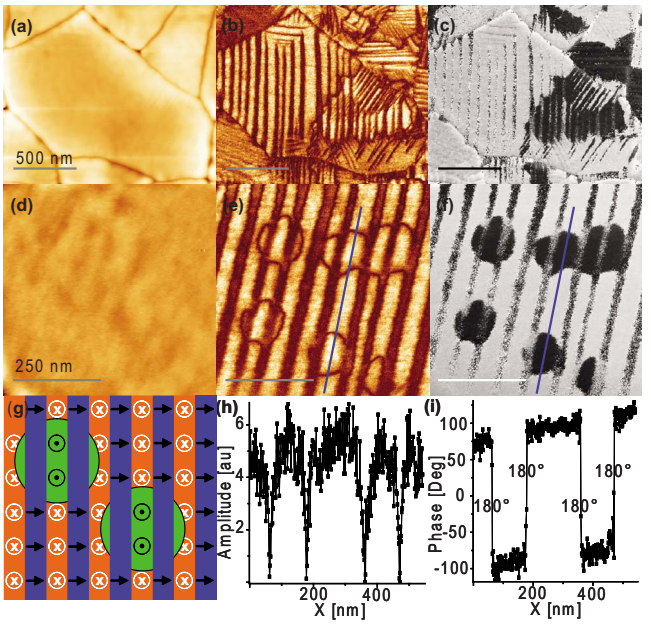

FIG. 1. (Color online) E-PFM imaging of local polarization switching in the center of a polytwin. Topography (a) and the simultaneously imaged E-PFM amplitude (b), and phase (c) of the native ferroelastic and ferroelectric domain distribution in a large grain in the sample. Topography (d) and the simultaneously imaged E-PFM amplitude (e), and phase (f) of a central area within the grain (the scan angle was slightly changed) after the polarization was switched locally at six different points with a voltage pulse applied through the tip. Stripes with alternating contrast at the two PFM images are periodic ferroelastic domains, whereas the 180° domains appear as close lines in the amplitude image and as areas with a high contrast in the phase image. This behavior suggests a dominancy of the piezoresponse over other possible contributions to the signal such as local and nonlocal electrostatic interactions and changes in the local modulus of elasticity. (g) Schematics of the area in [(d)–(f)] show the in-plane polarization in the *a* domains (blue stripes) and the homogeneous out-of-plane polarization in the *c* domains [white arrows go inside the lightly shaded (orange online) stripes] everywhere but in the engineered domains [dark arrows go outside in the medium shaded (green online) circular areas]. (h) A profile line of the amplitude image (marked in e) shows the signal arrives at the same valued in the opposite ferroelectric domains and (i) a profile line of the phase image (marked in f) shows the signal changes in 180° at the interface between ferroelectric domains, both supporting the fact that the potential electrostatic contribution is eliminated.

tionally, if changes in the local elastic modulus would have been significant, the signal obtained from the area around grain boundaries should have been dominant and even distort the image; however, this is not the case. This ultimately makes image interpretation relatively straightforward. In fact, the line profiles in Figs. 1(h) and 1(i) coincide with the description of negligible electrostatic contribution as was analyzed by Kalinin and Bonnell[19] and Figs. 1(e) and 1(f) are exactly the images one is expected to obtain with PFM, if the signal is almost purely piezoresponse.

Another issue that may affect PFM is related to in-plane vs out-of-plane domain imaging. This is accomplished by measuring the vertical and lateral deflection of the cantilever, respectively. In order to unequivocally detect these independently and rule out any crosstalk, it is important to ensure that the optics are optimally aligned. In the experiments presented below, the microscope was adjusted such that a vertical deflection of the cantilever was not detectable in the lateral detector and vice versa, thus avoiding the possibility of any crosstalk.

III. REVERSIBILITY OF DOMAIN SWITCHING

During the last few years, there have been several independent works in which the response of ferroelastic domains to external excitations was investigated. In the beginning, it was shown that under an applied electric field, individual elastic domain walls can move.[12] Later, it was demonstrated that the electric field can move several neighboring elastic domains.[10,11,22] Lastly, recent works presented that the elastic domain motion can, theoretically, be controlled to some extent.[23,24] Moreover, although it is well known how ferroelectric domains respond to electric fields, the interplay between ferroelectricity and ferroelasticity has remained obscured due to the lack of a suitable technique to study both simultaneously. Furthermore, although elastic domains can move under an electric field, it is not yet clear whether this motion is reversible. The behavior of ferroelastic domains during ferroelectric domain reversal is technologically significant, as many applications, such as nonvolatile memory devices are based on the reversibility of ferroelectric domains. Moreover, this is a fundamental question because if the elastic domain motion is not reversible they are *pseudoelastic* and only if it is reversible they are ferroelastic. In particular, some studies suggest that in some materials, the first motion is randomly determined but can be reversed with an opposite electric field.[22] On the other hand, as was mentioned above, it has also been claimed that the reorientation of the domains can be tuned only by selecting the appropriate path of the external electric field so that the domains are "dragged"[23,24] but it is not clear if this tuning is reversible. Therefore, we first wished to examine the reaction of ferroelectric and elastic domains to opposite electric fields and to explore the interplay between the two domain types.

For targeting this goal, we chose a 2 μm$\times$2 μm area that contains large grains with a rather homogeneous domain distribution and imaged it with E-PFM [Figs. 2(a)–2(c)]. In such an area, the effect of geometry is negligible so that the observations reflect the behavior of a single crystal. We then

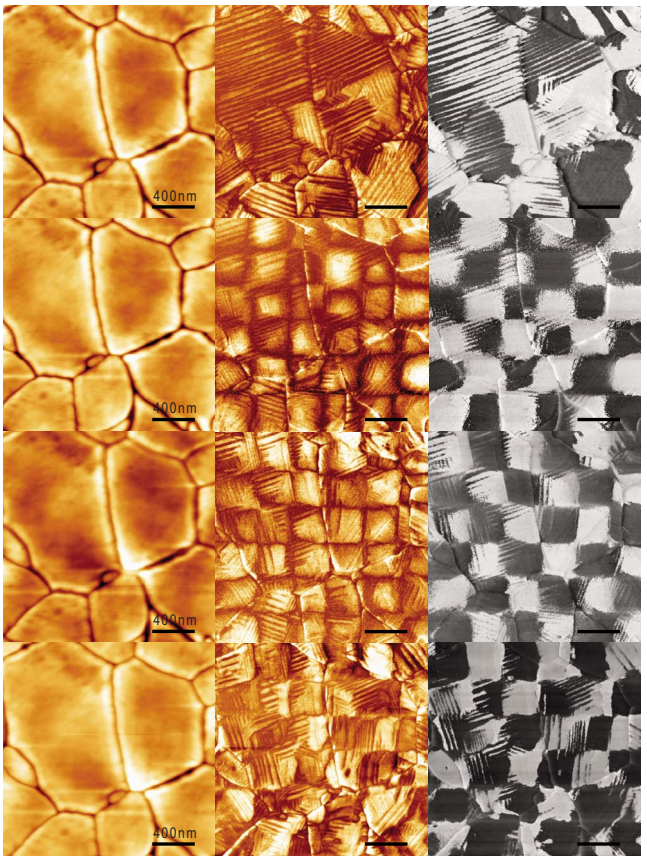

FIG. 2. (Color online) Nonreversible 90° domains within reversible 180° domains. [(a)–(c)] A topography, out-of-plane amplitude and phase, and in-plane phase E-PFM images of the native domain distribution in a granular area (left to right). [(d)–(f)] Topography, out-of-plane amplitude and phase E-PFM images of the same area after scanning the area while dividing it to 6$\times$6 squares and applying 10 V between the tip and the bottom electrode, whereas the polarity was changed when moving from one square to another. As a result, ferroelectric domains arranged in the form of a chessboard (phase) while the ferroelastic domain configuration has changed (amplitude). [(g)–(i)] Topography, out-of-plane amplitude and phase E-PFM images of the same area after scanning the area in the same manner as before while reversing the polarity in each square. The ferroelastic domains were reversed (phase), whereas the ferroelastic domains assumed a new configuration (amplitude). [(j)–(l)] Topography, out-of-plane amplitude and phase E-PFM images of the same area after scanning the area exactly in the same manner as in the first manipulation. The ferroelectric domains are back to their initial excited state (phase) while the ferroelastic domains arranged differently from all previous arrangements (amplitude).

scanned the area while dividing it into 6$\times$6 equal squares and applying opposite bias (+10 V and −10 V) at any two neighboring squares, forming a "chessboard" structure. The ensuing domain distribution was then mapped with E-PFM [Figs. 2(d)–2(f)]. The phase image [Fig. 2(f)] reveals that the macroscopic polarization (ferroelectric domains) followed the artificial chessboard patterning [Fig. 2(b)] while the ferroelastic domains [Fig. 2(e)] have changed in almost all of the ferroelectric domains, mainly by reorienting themselves. This is in agreement with recent studies that treat *bundles* of ferroelastic domains as individual entities (metaelastic do-

mains) that can form the macroscopic ferroelectric domains.[8] Next, to explore the influence of an opposite electric field we repeated exactly the same scan scheme as before while reversing the bias across the chessboard pattern. The outcome of this manipulation is shown in Figs. 2(g)–2(i). Indeed, the macroscopic polarization followed the patterning and has been reversed accordingly [Fig. 2(i)]. Nonetheless, a careful look at the amplitude image [Fig. 2(h)] reveals that the ferroelastic domains have changed once again to support the new ferroelectric domain distribution, supporting again the idea that bundles of ferroelastic stripes constitute the macroscopic polarization. Lastly, we scanned the area while applying the bias exactly in the same manner as in the first excitation (opposite to the previous scan) and imaged the resultant domain distribution [Figs. 2(j)–2(l)]. The resultant imaging shows that ferroelectric domains had been reversed again as expected [Fig. 2(l) phase, which is similar to the phase in Fig. 2(i)]. However, the ferroelastic domain distribution became different from what it was after each of the previous scans, as well as from the native structure [Fig. 2(k)]. In fact, it should be noted that repeating this process several more times, the ferroelastic domain distribution changed continuously and did not converge to any particular structure. Therefore, one can clearly deduce that ferroelectricity is completely reversible with reversed electric field, whereas ferroelasticity is not or at least not necessarily. Nonetheless, when ferroelectric domains are switched, the ferroelastic domains reorientate, probably to stabilize the net macroscopic polarization of the ferroelectric domains. An important outcome from this observed interplay between ferroelectricity and ferroelasticity is that the traditional treatment of ferroelectric domains as independent entities seems to be too naïve, as ferroelastic domains play an obvious major role in the dynamics of ferroelectricity and therefore cannot be neglected. Moreover, the two previously proposed mechanisms do not describe the switching mechanism under the framework of the current study, requiring an alternative explanation.

At this point, a natural explanation is that ferroelectric domains have only two possibilities to pick from: "up" or "down." On the other hand, the additional degrees of freedom of ferroelasticity makes the writing process irreversible as the domains can pick one of many possibilities, i.e., different angles of the stripes. These possibilities are finite as they are determined by the geometrical boundary conditions that are imposed, e.g., by the grain boundaries and by the crystallographic match between the different phases of the elastic domains between themselves as well as with the substrate. Therefore, the possible angles in which the bundles can rotate are discrete. At this point, one may presume that the different ferroelastic domain arrangements are close in energy and therefore each artificially made state is stable.

IV. RELAXATION MECHANISMS OF BUNDLE DOMAINS

In order to examine the stability of artificially formed domains, as well as to study the influence of boundary conditions on the switching mechanism in finite patterns., we conducted a different experiment in which their relaxation was examined.

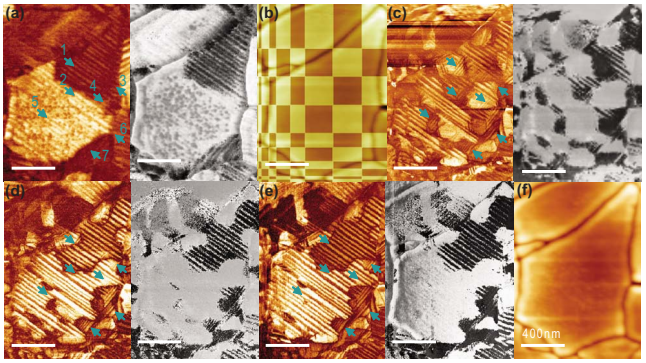

FIG. 3. (Color online) E-PFM imaging of engineered domains relaxation in a large grain in PZT film. (a) The native domain distribution in the large grain as detected with amplitude (left) and phase (right) E-PFM imaging (arrows and numbers are added to guide the eye tracking areas of interest). (b) The engineered patterns, superimposed on the topography—the area was scanned while applying 10 V (bright areas) and −10 V (dark areas) between the conducting scanning tip and the bottom Ir electrode. (c) The ferroelastic (left—amplitude) and ferroelectric (right—phase) engineered domain distribution—ferroelastic domains reorganized at most of the ferroelectric domain boundaries, as observed 780 s after the excitation. (d) and (e) show the domain relaxation in the area 1980 s and 72 h after the removal of the external dc field, respectively (left—amplitude and right—phase). (f) The topography of the area as imaged by atomic force microscopy is presented as a reference (all scale bars are 400 nm).

In Fig. 3(a), the native ferroelastic and ferroelectric domain distribution within a grain is shown. Periodic stripes (polytwins) perpendicular to the grain's long side occupy most of the grain, whereas the polarization in the *c* domains at the top of the grain is opposite to that of the bottom, as can be seen in the amplitude and phase images, respectively. The ferroelastic domain distribution complies with recent studies that report a tendency of the polytwins to align not parallel to the grain boundary.[8,25] Therefore, the bundle of stripe domains at the bottom right side that is perpendicular to the main orientation is not surprising, as the stripes there are still perpendicular to a local grain boundary (designated by "7"). Similar to the previous experiment, the large size of this grain suggests that its behavior should indicate the behavior of a single crystal. The concept of the experiment was to form a regular array of ferroelectric domains and observe their evolution as well as that of the ferroelastic domains therein. We divided the grain into small areas of different sizes and imaged it while applying +10 V or −10 V (above the dc coercive value of around 4 V) between the tip and the Ir bottom electrode as indicated in Fig. 3(b). As a result, the macroscopic out-of-plane polarization (i.e., the macroscopic ferroelectric domains that appear in the E-PFM phase image) formed the written structure as expected [right image in Fig. 3(c)]. Nonetheless, the amplitude image [left image in Fig. 3(c)] shows that although in some areas, the polarization was reversed in the *c* stripes, in many areas, the orientation (and in some cases, the periodicity) of the stripes had been altered, in agreement with previous studies,[10,11,22–24] as well as with

the above experiment. As was demonstrated above and has recently been shown, ferroelastic domains exist in ordered arrays, or bundles, that behave as independent elastic domains. This complies with the findings presented here in which macroscopic ferroelectric domains are formed with the aid of the modified bundle domains that are organized at the interface between opposite ferroelectric domains to act as mediators, as broadly discussed elsewhere.[8]

One probable explanation for this interplay between ferroelastic and ferroelectric switching is the possible high energy associated with the "head-to-tail" state, i.e., a state in which excess charge is accumulated within ferroelastic domain walls.[26,27] To avoid such a state, when the external electric field flips the polarization within the *c* domains, the polarization of the *a* stripes should also change accordingly. As a result, the bundles have the flexibility to reorganize into a different structure that may differ from the original structure in orientation. If there is an associated change in the magnitude of the local shear strain due to the switching, the ferroelastic domains will also change their width, as strain is released perpendicular to the stripes along the axis in which the unit-cell orientation is alternating.[28,29]

At this stage, we have not yet discussed the driving mechanism that determines the bundle reorganization (change in domain width and orientation) but it will broadly fall into one of the following classes: (a) the original and final ferroelastic domain distributions have the same energy but with an energy barrier between them (i.e., a process that is reminiscent of the glass transition) and (b) they have different energy. For (a), under the external electric field, excess charge is accumulated at the domain walls and cannot be neutralized. Furthermore, strain is also induced due to the electromechanical coupling of the system (piezoelectricity). Thus, when the electric field is large enough, the bundle is excited above the energy barrier and randomly picks one of the similar energy structures. The possibilities for the orientation of the stripes are discrete, restricting how strain can be released. In the absence of any dramatic geometrical influence (e.g., as in the case of large grains), these possibilities are determined by the crystallographic orientation of both the seeding layer and the ferroelectric film, as well as by the matching between the two and by the matching between the different elastic domains. When the excitation is removed, the bundle remains in that structure which can differ from the original state in orientation and domain width. In this case, both the native and final states are at an energy minimum and therefore should be stable. In the second possible scenario (b), the free energy of the original and final states is different. The former is the minimum-energy state in the absence of external perturbations, whereas the latter arises to accommodate the uncompensated strain and domain-wall charging, induced by the excitation. That is, the orientation and periodicity of the perturbed bundles is determined by the manner in which the electric field is applied. In this case, when the excitation is removed, the ferroelastic domain distribution, which was stable under the excitation, is not necessarily a minimum-energy state any more. Moreover, the stronger the excitation, the higher the energy of the excited state which in turn will be more unstable higher on removal of the excitation. Hence, when the excitation is strong, the excited state is expected to relax into a more stable state upon its removal, whereas the relaxed state should be similar to the original domain distribution or to another minimum energy of the unperturbed state.

Since the final state is stable in the first case, (a), whereas it is unstable in the second case, (b), by following the relaxation of the written patterns, it should be possible to determine which mechanism is responsible for relaxation. In order to explore the stability of the written patterns, we imaged the domain distribution at different times after the excitation removal. The ferroelectric (phase) and ferroelastic (amplitude) domain distribution of the same area was then recorded 1980 s after Fig. 3(c) was imaged, as presented in Fig. 3(d) (right and left images, respectively), whereas it should be noted here that Fig. 3(c) was completed 780 s after the excitation was removed. One can clearly see that in many areas (the arrows denoted by "1-3"), the ferroelastic domains returned to their original distribution, whereas the macroscopic ferroelectric domains had relaxed as well. It is interesting to note that in these areas, the 180° domains remained reversed even without having the mediating bundles.[8] That is, these areas returned to their original state and the polarization was reversed in the middle of the *c* domain stripes within the polytwins. On the other hand, in some areas, the written bundles either remained unchanged (arrows "6-7"), or shrunk (arrows "4-5"). The area was then imaged continuously during the next 3 days. The written domains in the areas designated by "4" and "5" vanished soon while no other apparent changes occurred, as can be seen in Fig. 3(e) (the 26th scan, after 72 h). In other words, after the excitation was removed, the ferroelastic domains relaxed to an equilibrium state over a period of approx 10^3 s, with little or no change detected beyond that, as measured to 10^5 s.

The empirical Arrhenius equation describes the relaxation rate K.[30] Since the relaxation time satisfies $\tau = K^{-1}$, the Arrhenius equation can be rewritten as

$$\tau = \tau_0 \exp(E_a/k_B T), \tag{1}$$

where E_a is the activation energy or the potential barrier of the excited state, k_B is the Boltzmann constant, and τ_0 depends on both the material and temperature (T).[30] The fact that no apparent changes were observed after $\sim 10^3$ s indicates that to first order, this is the approximate relaxation-time constant of the system. Previous studies on PZT under ambient conditions (i.e., similar τ_0) show that the relaxation-time constant of 180° domains in the presence of 90° domains is on the order of $\tau \approx 10^5$ s.[24] The two orders of magnitude difference between the relaxation time of 90° and 180° domains implies that the two relaxation mechanisms are different in their nature, in accordance with the fact that the process of 90° domain switching includes an additional mechanical influence. Based on the data presented in previous works,[30,31] $\tau_0 \approx 10^5$ s for PZT at room temperature. Hence, from Eq. (1), one can extract the difference in the activation energy between the two mechanisms: $E_{a\_180°}/E_{a\_90°} = \ln(\tau_{180°}/\tau_0)/\ln(\tau_{90°}/\tau_0) \approx 2$. Namely, the potential barrier confining a written 180° domain is about twice as high as the potential barrier of a written 90° domain.

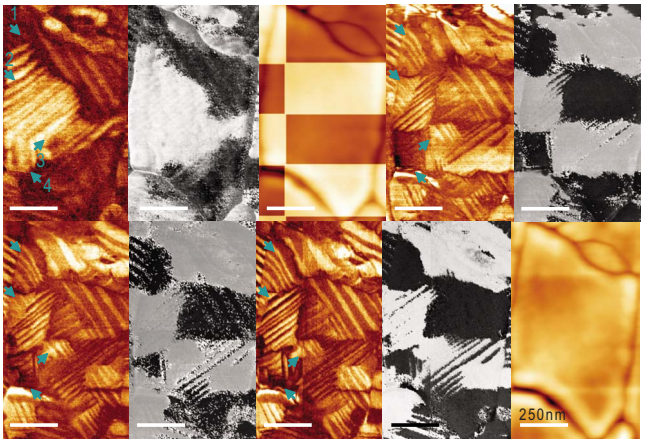

FIG. 4. (Color online) E-PFM imaging of engineered domains relaxation in a smaller grain in PZT film. (a) The native domain distribution in the small grain as detected with amplitude (left) and phase (right) E-PFM imaging (arrows and numbers are added to guide the eye tracking areas of interest). (b) The engineered patterns, superimposed on the topography—the area was scanned while applying 10 V (bright areas) and −10 V (dark areas) between the conducting scanning tip and the bottom Ir electrode, as detected 780 s after the writing process was complete. (c) The ferroelastic (left—amplitude) and ferroelectric (right—phase) engineered domain distribution—ferroelastic domains reorganized at most of the ferroelectric domain boundaries. (d) and (e) show the domain relaxation in the area 2760 and 6660 s after the removal of the external dc field, respectively (left—amplitude and right—phase). (f) The topography of the area as imaged by atomic force microscopy is presented as a reference (all scale bars are 250 nm).

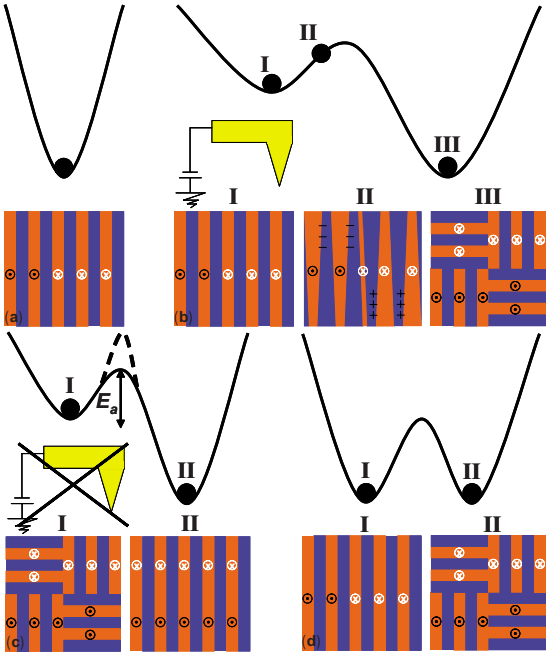

FIG. 5. (Color online) Schematic energetic profile of 90° domain relaxation. (a) When cooled below the Curie temperature, the ferroelectric material is organized into its native ferroelectric and ferroelastic domain distribution. (b) When an external electric field, E_a is introduced during the writing process, the native state (i) is not any more the lowest energy state, due to the induced charge and strain (II). Therefore, if the excitation is above a certain energy value, the ferroelastic domains will organize into a lower energetic state (III). (c) Removing the perturbation, the new state becomes unstable (i) and the ferroelastic domains return to their original native state (II), in a time constant that depends on E_a. However, the polarization (ferroelectric domains) of this state can differ from the original distribution, i.e., there is a "memory effect" of the ferroelastic domain relaxation. In the case of smaller grains, the engineered ferroelastic domain distribution is stable due to either a high potential barrier that slows down the relaxation (dashed line in c) or because the final state is of the same energy as the original one, due to the effect of boundary conditions (I and II in d).

The observed relaxation of the bundle domains indicates that the reorientation of the bundles under the applied electric field is an unstable state, which relaxes into a stable state that is almost identical to the original ferroelastic domain distribution, although the switched ferroelectric (180°) domain distribution can be stable. Therefore, our observation supports the second mechanism [i.e., (b)] proposed above, suggesting that the 90° domains reorganization occurs only to reduce the free energy when the electric field is being applied. When the excitation is removed, the new state is unstable and decays to the initial domain distribution or one of similar energy.

The next step was to explore the influence of local geometry on the stability of the excited domains. Therefore, we looked also at the domain relaxation within a smaller grain that was excited and observed in the same manner as the larger grain, as demonstrated in Fig. 4. One can see that in the smaller grain, under the electric field, the ferroelastic domains organized similarly to the way they did in the larger grain, i.e., reoriented to allow field closure and to act as mediators at the boundaries of the macroscopic ferroelectric domains. Nevertheless, in this case, the excited ferroelastic domains remained pinned and did not relax to their original state after a long time. The dependence of the relaxation on the grain size, that is presented in Figs. 3 and 4 represents the typical behavior we have observed in our experiments. For instance, the area in Fig. 1 was imaged a long time after the last excitation and the elastic domains have returned to their original state. In fact, this dependence on grain size complies with recent works that link the ferroelastic domain distribution with the grain size.[8,32] It has also been shown that grains with a lateral size equal to or smaller than the film thickness usually tend to have only a single bundle domain, i.e., a single coherent striped domains structure. It should be noted that we saw that when such thin grains are excited, the entire bundle is rotated into a different orientation and the resultant bundle remains unchanged a long while ($\geqslant 10^3$ s) after the excitation removal. Moreover, we saw that the smallest ferroelectric domains that were successfully written by a switched bundle is of a typical lateral size of ~80 nm, which is comparable with the film thickness.

Based on the above, the driving mechanism of the ferroelastic domain relaxation can be described as follows: (a) when undergoing the ferroelectric phase transition, the grain is split into elastic domains; (b) under an external electric field, the native domain distribution is excited due to strain and uncompensated charge at the domain walls; (c) when the

excitation corresponds to energy that is higher than a certain threshold value and over the area that is larger than the film thickness, the elastic domains are excited and free to move; (d) the domains reorganize into a new structure that minimizes the free energy under the perturbing electric field; and (e) when the excitation is removed, the domains may or may not relax, depending on the geometrical constraints: (1) in the absence of dramatic geometric boundary conditions (e.g., in the center of large grains), the domains will relax into a structure that is similar to the original distribution, which is likely to be an absolute free-energy minimum state and (2) in the presence of geometrical constraints (e.g., small grains), the domains generally remain pinned. This may occur due to one of two reasons: (i) the free energy of the final domain distribution is close to that of the original state, i.e., the free energy is at its minimum in both cases or (ii) the geometrical boundary conditions increase the energy threshold of domain reorganization. Therefore, although the free energy of the new domain distribution is only at a local minimum and not at an absolute one, the energy needed to exit this state is too high to occur spontaneously, making the state metastable. A summary of the entire mechanism is illustrated in Fig. 5.

Figure 3 indicates that when a ferroelectric domain is switched with a scanning tip at a scale larger than the film thickness, the ferroelastic domains are also switched to support the new state, probably by preventing a head-to-head state. On the other hand, Fig. 3 demonstrates that in finite structures, the ferroelectric domains can be switched in the middle of the bundle. This indicates that the elastic interactions contribute to the energy more than the electric interactions. Finally, Fig. 1 shows that when a ferroelectric domain is switched at the center of the bundle by applying a pulse with a stationary tip, the ferroelastic domains remain unchanged, even at the cost of a head-to-head state. The behavior of the domains in Fig. 1 may have two possible explanations. First, the diameter of the tip is much smaller than the film thickness so that the electric field applied by the tip is attenuated rather close to its center. This means that the energy of the excitation is concentrated in an area that is much smaller than the film thickness and the ferroelectric domains in Fig. 1 are much smaller than the bundle surrounding it. Therefore, even if the electric part of the energy is reduced when the excess charge of the head-to-head state is compensated, the mechanical part of the energy involved with a formation of such a small bundle is probably too high. That is, in this mechanism, the electric part is dominant over the contribution of the elasticity to the energy. Second, Balke *et al.*[23] have recently suggested that when a voltage is applied on the sample through a scanning tip, the elastic domains may be dragged by the tip, whereas this is not possible with a stationary tip (they explored a multiferroic material in the rhombohedral state but the concept may be used also in ferroelectric ferroelastic systems). Nevertheless, a conclusive explanation for the origin of this difference is not yet clear.

V. CONCLUSIONS

To conclude, we demonstrated here how ferroelastic domains are organized under an electric field at a low scale (within the ferroelastic stripes) as well as at the intermediate scale (at the scale of the bundles). We discussed the stability of the written domains (at the intermediate scale) and we demonstrated how they relax as well as how the relaxation depends on geometrical conditions, and we proposed different switching mechanisms for both single-crystal-like structures and finite patterns. Finally, we showed that under opposite electric field, ferroelectric domains are reversible, whereas ferroelastic domains are not, and we illustrated that the ferroelastic domain distribution controls the previously reported macroscopic ferroelectric domain engineering in simple multiferroic systems, which constitutes the basis of, e.g., ferroelectric-based memory devices.

ACKNOWLEDGMENTS

This work was carried out as part of the Nokia-University of Cambridge collaboration in Nanotechnology. Image processing was carried out using WSXM (Ref. 33). Y.I. would also like to thank AJA, the Wingate Foundation, FCO, AIA, and Bn'ai Brith for financial support.

*Corresponding author; yachinivry@gmail.com
†Corresponding author; cd229@eng.cam.ac.uk

[1] J. F. Scott, Science **315**, 954 (2007).
[2] M. Dawber, K. M. Rabe, and J. F. Scott, Rev. Mod. Phys. **77**, 1083 (2005).
[3] N. Setter, D. Damjanovic, L. Eng, G. Fox, S. Gevorgian, S. Hong, A. Kingon, H. Kohlstedt, N. Y. Park, G. B. Stephenson, I. Stolitchnov, A. K. Taganstev, D. V. Taylor, T. Yamada, and S. Streiffer, J. Appl. Phys. **100**, 051606 (2006).
[4] C. L. Jia, S. B. Mi, K. Urban, I. Vrejoiu, M. Alexe, and D. Hesse, Nature Mater. **7**, 57 (2008).
[5] F. Jona and G. Shirane, *Ferroelectric Crystals* (Dover, New York, 1993).
[6] J. Y. Li, R. C. Rogan, E. Ustundag, and K. Bhattacharya, Nature Mater. **4**, 776 (2005).
[7] R. Ramesh and D. G. Schlom, Science **296**, 1975 (2002).
[8] Y. Ivry, D. P. Chu, and C. Durkan, Nanotechnology **21**, 065702 (2010).
[9] Y. Ivry, V. Lyahovitskaya, I. Zon, I. Lubomirsky, E. Wachtel, and A. L. Roytburd, Appl. Phys. Lett. **90**, 172905 (2007).
[10] G. Le Rhun, I. Vrejoiu, and M. Alexe, Appl. Phys. Lett. **90**, 012908 (2007).
[11] G. Le Rhun, I. Vrejoiu, L. Pintilie, D. Hesse, M. Alexe, and U. Gösele, Nanotechnology **17**, 3154 (2006).
[12] V. Nagarajan, A. Roytburd, A. Stanishevsky, S. Prasertchoung, T. Zhao, L. Chen, J. Melngailis, O. Auciello, and R. Ramesh, Nature Mater. **2**, 43 (2003).
[13] A. Roelofs, N. A. Pertseva, R. Waser, F. Schlaphof, L. M. Eng, C. Ganpule, V. Nagarajan, and R. Ramesh, Appl. Phys. Lett. **80**, 1424 (2002).

[14] Y. Ivry, D. P. Chu, and C. Durkan, Appl. Phys. Lett. **94**, 162903 (2009).
[15] K. Nishi, A. Usui, and H. Sakaki, Appl. Phys. Lett. **61**, 31 (1992).
[16] A. Gruverman, O. Auciello, and H. Tokumoto, J. Vac. Sci. Technol. B **14**, 602 (1996).
[17] C. Durkan, M. E. Welland, D. P. Chu, and P. Migliorato, Phys. Rev. B **60**, 16198 (1999).
[18] A simple calculation shows that the soft cantilever bends downward toward the sample with a peak amplitude of less than an angstrom.
[19] *Nanoscale Characterisation of Ferrorlectric Materials*, edited by M. Alexe and A. Gruverman (Springer-Verlag, Heidelberg, 2004).
[20] U. Rabe and W. Arnold, Appl. Phys. Lett. **64**, 1493 (1994).
[21] U. Rabe, M. Kopycinska, S. Hirsekorn, J. M. Saldana, G. A. Schneider, and W. Arnold, J. Phys. D **35**, 2621 (2002).
[22] V. Anbusathaiah, D. Kan, F. C. Kartawidjaja, R. Mahjoub, M. A. Arredondo, S. Wicks, I. Takeuchi, J. Wang, and V. Nagarajan, Adv. Mater. **21**, 3497 (2009).
[23] N. Balke, S. Choudhury, S. Jesse, M. Huijben, Y. H. Chu, A. P. Baddorf, L. Q. Chen, R. Ramesh, and S. V. Kalinin, Nat. Nanotechnol. **4**, 868 (2009).
[24] H. Béa, P. Paruch, M. Bibes, and A. Barthélémy, arXiv:0907.4568 (unpublished).
[25] A. Schilling, D. Byrne, G. Catalan, K. G. Webber, Y. A. Genenko, G. S. Wu, J. F. Scott, and J. M. Gregg, Nano Lett. **9**, 3359 (2009).
[26] C. S. Ganpule, V. Nagarajan, B. K. Hill, A. L. Roytburd, E. D. Williams, R. Ramesh, S. P. Alpay, A. Roelofs, R. Waser, and L. M. Eng, J. Appl. Phys. **91**, 1477 (2002).
[27] W. J. Merz, Phys. Rev. **95**, 690 (1954).
[28] A. L. Roytburd, Phys. Status Solidi A **37**, 329 (1976).
[29] A. Schilling, T. B. Adams, R. M. Bowman, J. M. Gregg, G. Catalan, and J. F. Scott, Phys. Rev. B **74**, 024115 (2006).
[30] C. S. Ganpule, A. L. Roytburd, V. Nagarajan, B. K. Hill, S. B. Ogale, E. D. Williams, and R. Ramesh, Phys. Rev. B **65**, 014101 (2001).
[31] L. H. Hamedi, M. Guilloux-Viry, A. Perrin, and G. Garry, Thin Solid Films **352**, 66 (1999).
[32] T. Hoshina, H. Kakemoto, T. Tsurumi, S. Wadaa, and M. Yashima, J. Appl. Phys. **99**, 054311 (2006).
[33] I. Horcas, R. Fernandez, J. M. Gomez-Rodriguez, J. Colchero, J. Gomez-Herrero, and A. M. Baro, Rev. Sci. Instrum. **78**, 013705 (2007).